Surface Science 172 (1986) 733–753
North-Holland, Amsterdam

AN EELS AND TPD STUDY OF THE ADSORPTION AND DECOMPOSITION OF ACETIC ACID ON THE Al(111) SURFACE

J.G. CHEN *, J.E. CROWELL and J.T. YATES, Jr.

Surface Science Center, Department of Chemistry, University of Pittsburgh, Pittsburgh, Pennsylvania 15260, USA

Received 30 December 1985; accepted for publication 14 February 1986

The adsorption and decomposition of acetic acid on Al(111) have been studied using electron energy loss spectroscopy (EELS), temperature programmed desorption (TPD), and Auger electron spectroscopy (AES). Acetic acid reacts with clean Al(111) at 120 K to form a surface acetate species. The adsorbed acetate bonds to the surface in a symmetric configuration with C_s symmetry at 120 K. The adsorption of molecular acetic acid occurs at this temperature only after saturation of the surface acetate layer; this physisorbed multilayer desorbs molecularly at 167 K. Thermal decomposition of the adsorbed acetate leads to a carbon- and oxygen-covered surface; the only detectable thermal decomposition product is H_2. Electron irradiation induces a similar decomposition process of the surface acetate.

1. Introduction

The adsorption and decomposition of acetic acid on transition metal single crystal surfaces have been the subject of several experimental investigations [1–5]. On the clean surfaces of Pt(111) [1], Cu(100) [2,3], and Cu(110) [5] at low temperatures (< 225 K), acetic acid adsorbs in a molecular form. Acetate species can be produced on these metal surfaces by either heating the adsorbed molecular acetic acid above 225 K [1–5] or by dosing oxygen onto the surfaces prior to the adsorption of acetic acid [1,5]. The major thermal decomposition products observed from adsorbed acetate on these metal surfaces are CO, CO_2, and H_2.

The interaction of atomically-clean aluminum single crystal surfaces with adsorbates other than oxygen is virtually unexplored at present. Due to the high affinity of Al surfaces toward oxygen [6] and its known reactivity toward O–H bond scission [7], one would predict the formation of acetate on Al(111)

* Andrew Mellon Predoctoral Fellow.

to be much easier than on transition metal surfaces. In addition, the strong reactivity of Al surfaces toward oxygen and carbon may lead to different decomposition products compared to those obtained by the decomposition of acetate on transition metals. Our interest in studying the interaction of acetic acid with Al(111) is to obtain a fundamental understanding of the reactivity of Al surfaces toward this class of organic molecules.

In our study, we have used electron energy loss spectroscopy (EELS), temperature programmed desorption (TPD), and Auger electron spectroscopy (AES) to characterize the adsorption and decomposition of acetic acid on Al(111) in the temperature range of 120–700 K. The adsorption of both CH_3COOH and CD_3COOH was investigated. In addition, the thermally-induced and electron-stimulated decomposition of the adsorbed species were studied to elucidate the decomposition pathway for surface acetate.

2. Experimental methods

The experiments reported here were carried out in a three level stainless steel UHV chamber with a typical base pressure of less than 1×10^{-10} mbar. A detailed description of the chamber and the preparation of the Al(111) single crystal has been given in a previous publication [8].

The EEL spectra in this work were collected at an incident beam energy of 2–3 eV. Typical resolution from a submonolayer acetic acid-dosed Al(111) surface was 60–100 cm^{-1} with an elastic peak intensity of 10^5 counts/s.

TPD data were measured by a shielded and pumped quadrupole mass spectrometer operating with a filament emission current of 2.0 mA and a multiplier voltage of 3.0 kV. The mass spectrometer was multiplexed using an IBM microcomputer and a Technivent interface, permitting one to monitor the time and temperature dependence of several masses, simultaneously. The temperature programming of the crystal was achieved using a programmable power source of our own design [9].

The Al(111) crystal was cleaned in situ after each set of experiments by repeated cycles of argon sputtering at 300 K and prolonged annealing at 700 K. The clean Al(111) surface was characterized by both AES and EELS.

The introduction of gases onto the Al(111) surface was carried out using a translatable molecular beam doser containing a capillary-array collimator [10]. The typical acetic acid pressure behind the internal 2 μm diameter doser orifice was 10 Torr, and the flux rate through the doser orifice was 3.0×10^{14} molecules $s^{-1}\,cm^{-2}$.

The reagents used in these experiments, CH_3COOH (99.9% purity, Baker Chemical Co.) and CD_3COOH (99.2 at% D, MSD Isotopes), were transferred to storage ampoules under a high purity nitrogen atmosphere and were then

purified using freeze–pump–thaw cycles in vacuum followed by either a double (CH_3COOH) or a triple (CD_3COOH) vacuum distillation.

3. Results

3.1. Adsorption of acetic acid on Al(111) at 120–130 K

A set of vibrational spectra recorded as a function of increasing CH_3COOH exposure on Al(111) at 121 K is shown in fig. 1. Initially, at an exposure of 3.2×10^{16} molecules/cm^2, three intense vibrational modes at 425, 675 and 1460 cm^{-1}, and a weak band at ≈ 2990 cm^{-1} are observed. The peak shapes and frequencies of the three intense loss features remain fairly constant and their intensities increase as the acetic acid exposure is increased to 6.3×10^{16} molecules/cm^2 (notice the 3-fold decrease in the scale expansion factor between spectra a and b). Also in spectrum 1b, a relatively weak band at 1055 cm^{-1} becomes visible. At higher CH_3COOH exposures, dramatic changes occur in the EEL spectra. After an exposure of 9.5×10^{16} molecules/cm^2 (spectrum 1c), in addition to those features observed at low CH_3COOH doses, some new vibrational modes start to develop. These are: a broad band at 990 cm^{-1}, a shoulder at ≈ 1350 cm^{-1}, and a mode at 1740 cm^{-1}. These new features become very intense and another band at 2740 cm^{-1} is observed at a CH_3COOH exposure of 1.5×10^{17} molecules/cm^2 (spectrum 1d).

A series of EEL spectra measured at 118–127 K as a function of increasing CD_3COOH exposure are plotted in fig. 2. The vibrational spectra recorded at low CD_3COOH exposures, spectra 2a and 2b, are quite similar to those observed in fig. 1 for the same range of acetic acid exposures. Spectra 1b and 2b are almost identical in the energy region below 2000 cm^{-1}, confirming that the three intense and one weak vibrational transitions observed below 2000 cm^{-1} are not due to motions involving C–H or C–D. The only difference observed between figs. 1b and 2b upon the partial deuteration is the frequency shift of the vibrational mode at 3010 cm^{-1} for CH_3COOH to 2285 cm^{-1} for CD_3COOH, as expected for the ν(C–H) and ν(C–D) modes, respectively. In the same fashion as observed in fig. 1, new modes begin to grow in at higher CD_3COOH exposures. By comparing spectra 2d and 1d, the differences are the appearance of new features at 1050, 2155 and 2275 cm^{-1}. In addition, the strongly overlapping losses centered near 1450 cm^{-1} in fig. 1d are much better resolved into two features at 1310 cm^{-1} and 1460 cm^{-1} in fig. 2d.

Both fig. 1 and fig. 2 show the same trend as the acetic acid exposure increases. At low acid exposures ($\leqslant 6.3 \times 10^{16}$ molecules/cm^2), five vibrational transitions are observed, three intense losses and two much weaker vibrational transitions. Only one of these modes involves C–H or C–D

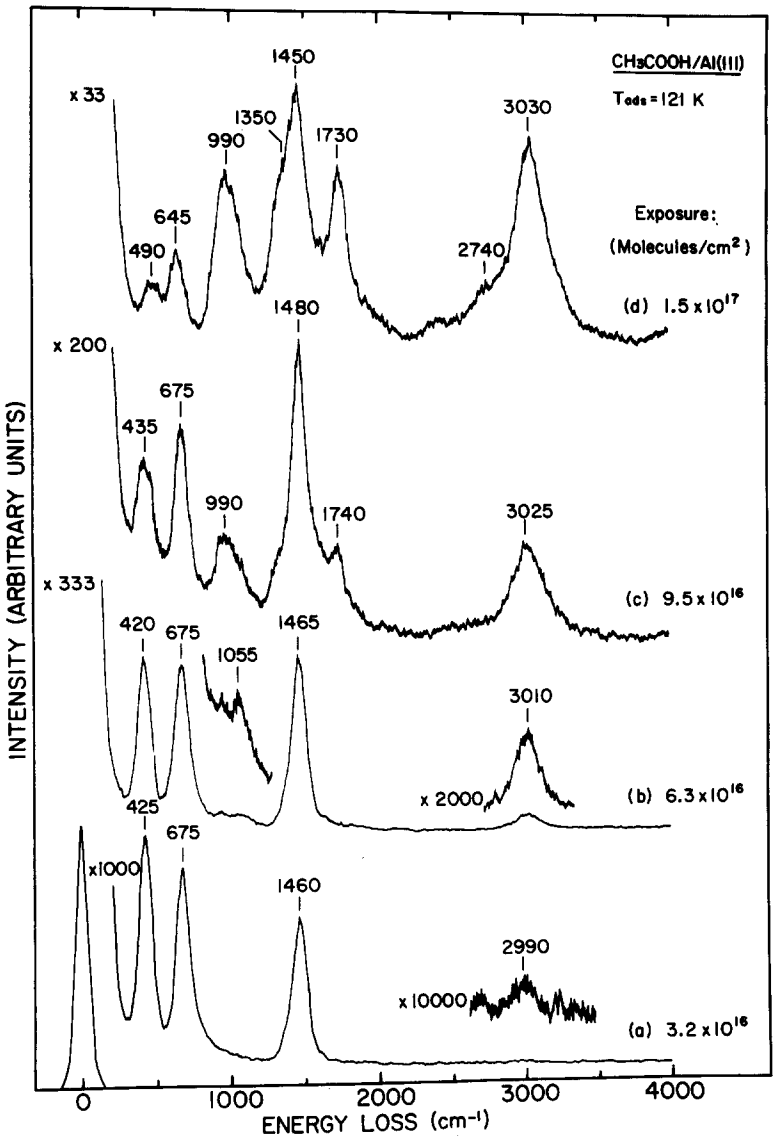

Fig. 1. Acetic acid adsorption on Al(111) at 121 K as a function of increasing CH_3COOH exposure.

motions; the four losses occurring below 2000 cm^{-1} involve C–C, C–O, Al–O or Al–C vibrations. Substantial spectral changes occur at higher acetic acid exposures. New features start to develop and become dominant at very high

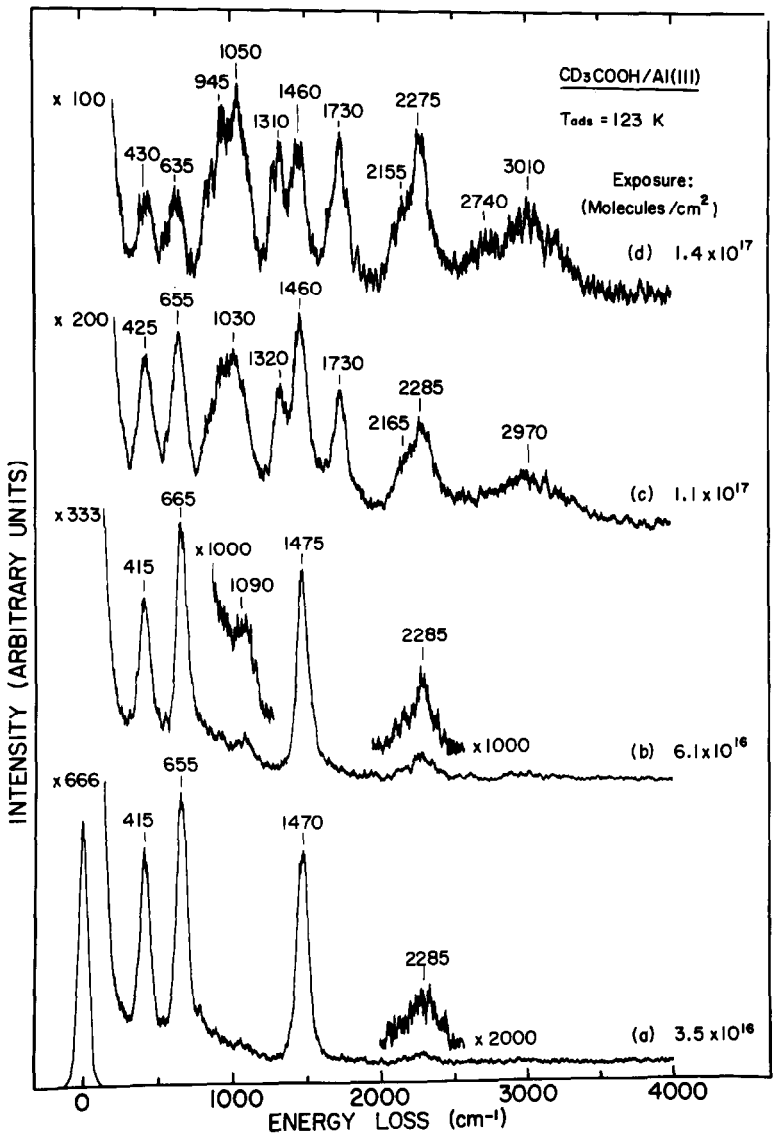

Fig. 2. EEL spectra collected as a function of increasing CD_3COOH exposure at 123 K.

acetic acid exposure (spectra 1d and 2d), but the three intense features initially observed remain visible in the spectra. The presence of a new adsorption species is suggested based on the abrupt spectral changes observed (in figs. 1 and 2) at higher acetic acid exposures.

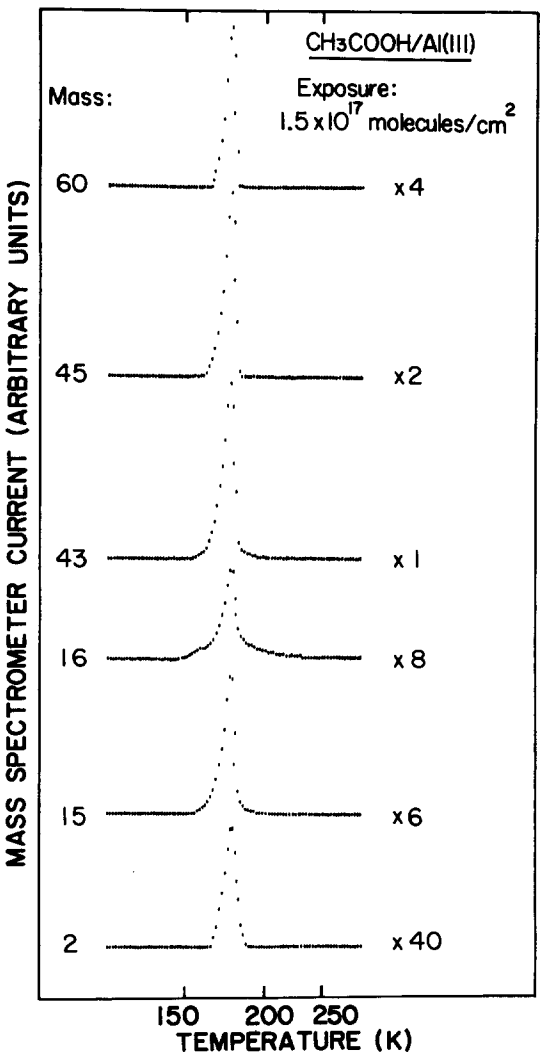

Fig. 3. Temperature programmed desorption (TPD) results for a condensed acetic acid layer for the temperature range of 134–250 K.

3.2. Thermal decomposition of the adsorbed species

The effect of heating the adsorbed species produced on Al(111) at low and high CH_3COOH exposures was also studied. The TPD data shown in fig. 3 were collected after an adsorbed layer was prepared by a relatively high CH_3COOH exposure, 1.5×10^{17} molecules/cm^2, at 134 K. This layer has an

EEL spectrum similar to that shown in fig. 1d. As shown in fig. 3, several different masses, 60, 45, 43, 16, 15, and 2 amu, display a desorption feature at 167 K. The desorption signal at 43 amu always exhibits the most intense peak in this range of CH_3COOH exposures.

TPD data collected from an adsorbed layer with a similar EEL spectrum to that shown in fig. 1c are given in fig. 4A. From the vibrational spectrum (fig.

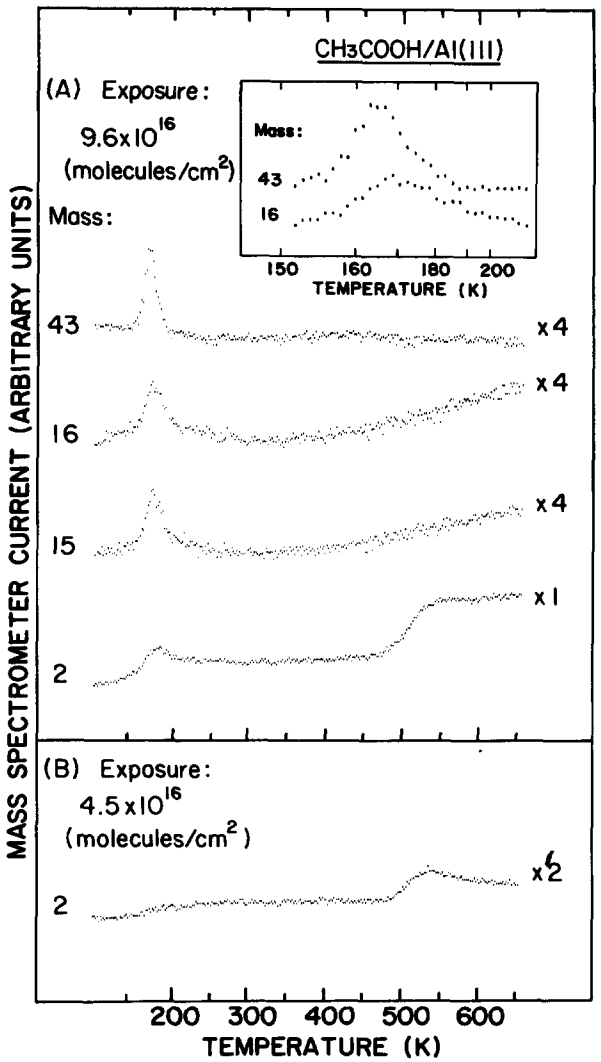

Fig. 4. TPD spectra for an adsorbed layer (A) with both acetate and condensed acetic acid (A), and (B) for only adsorbed acetate.

1c) one can see that at this CH_3COOH exposure, some new features in addition to those observed at low acetic acid exposures are just beginning to develop. In fig. 4A, desorption features at 43, 16, 15 and 2 amu evolve at 167 K as is observed in fig. 3, but with different peak ratios. The inset in fig. 4A reveals the slightly different shapes of the low temperature peaks at 43 and 16 amu. The only desorption feature observed above this temperature is a broad desorption state centered at 540 K due to H_2 evolution. A similar state is also observed at higher acetic acid exposures; this feature is not shown in fig. 3.

The TPD spectrum for an adsorbed layer on Al(111) at a lower CH_3COOH exposure, 4.5×10^{16} molecules/cm^2, is given in fig. 4B. The only detectable decomposition species at this exposure level is H_2, evolving at 540 K. The vibrational spectrum of this adsorbed layer is similar to that shown in fig. 1b.

A series of EEL spectra collected as a function of the Al(111) crystal temperature reached in a heating sequence are shown in fig. 5. Spectrum 5a was recorded following an acetic acid exposure of 1.5×10^{17} molecules/cm^2 at 121 K. The subsequent EELS measurements were performed at temperatures between 120 and 140 K after the adsorbed layer was momentarily heated to the indicated temperature. Upon warming to 200 K (spectrum 5b), the loss features at 990, 1730 and 2740 disappear, and new modes at 1050 and 1615 cm^{-1} begin to develop. Between 200 and 500 K (spectra 5b–5d), the EEL spectra in the energy region above 1000 cm^{-1} change only slightly, while a broad asymmetric feature develops between 500 and 900 cm^{-1}. By 700 K, all vibrational modes observed at 120 K have disappeared, and the loss features in the low energy region develop into a broad band at 850 cm^{-1} with a shoulder at 675 cm^{-1}.

EEL spectra representative of oxygen adsorption on Al(111) for a similar heating sequence as discussed above are shown in fig. 6. The adsorbed layer was prepared by an oxygen exposure of 3.5×10^{16} O_2/cm^2 at 122 K. At 200 K, the EEL spectrum is characterized by two loss features at 565 and 845 cm^{-1}, respectively. The systematic changes observed with increasing crystal temperature are the preferential increase of the higher frequency mode, the appearance of a new vibrational feature at 405 cm^{-1} at 500 K, and the slight frequency shift for all the vibrational transitions to higher energies.

By comparing figs. 5 and 6, one can see that the general mode development and frequency shift with temperature are quite similar in the energy region below 1000 cm^{-1}, except that the vibrational modes in fig. 6 are much better resolved.

A set of EEL spectra collected as a function of temperature for an adsorbed layer prepared at a lower CH_3COOH exposure than that of fig. 5 is reproduced in fig. 7. The spectrum collected at 200 K (spectrum 7a) is identical to that obtained at 123 K (not shown). At temperatures above 200 K, the systematic changes observed upon heating are a gradual decrease in intensity of the features observed at 200 K, and the development of a new broad feature

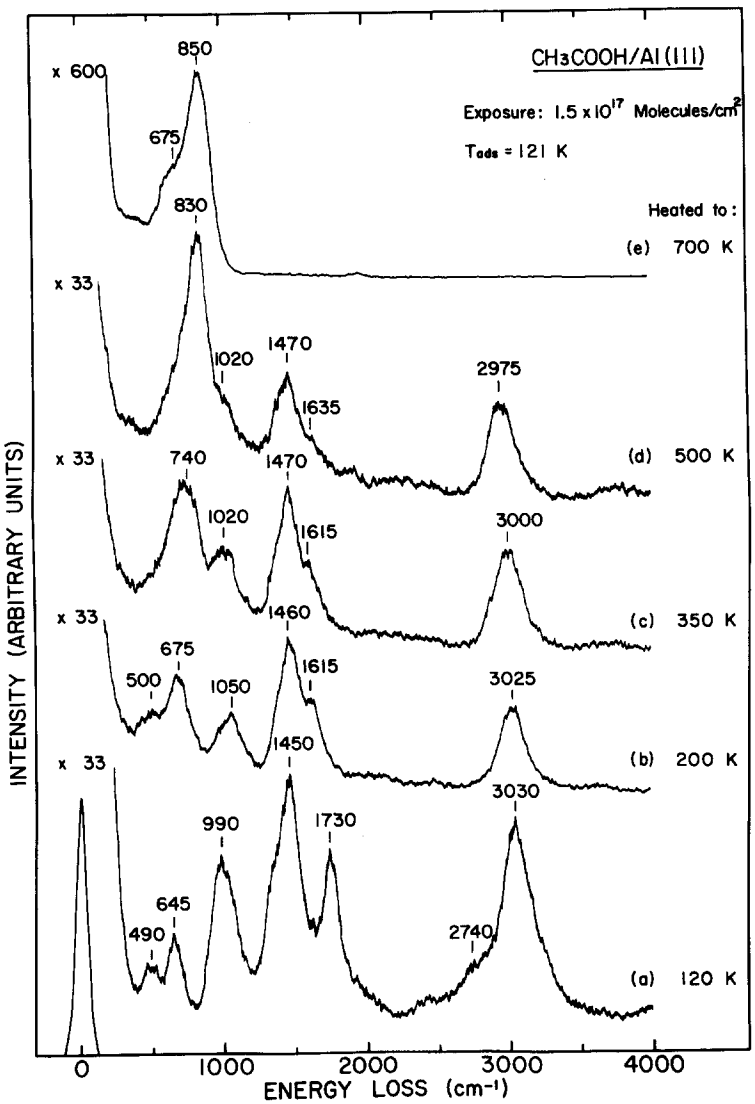

Fig. 5. EEL spectra of a condensed acetic acid layer on Al(111) recorded as a function of increasing crystal temperature. All measurements were performed at 120–140 K.

at ≈ 735 cm^{-1}. By 700 K, all vibrational modes disappear except the asymmetric broad band centered at 840 cm^{-1} with a shoulder at 660 cm^{-1}, which is quite similar to that obtained upon heating a high coverage layer to the same temperature (fig. 5e). The changes observed in fig. 7 in the energy region below 1000 cm^{-1} are again analogous to those measured for the

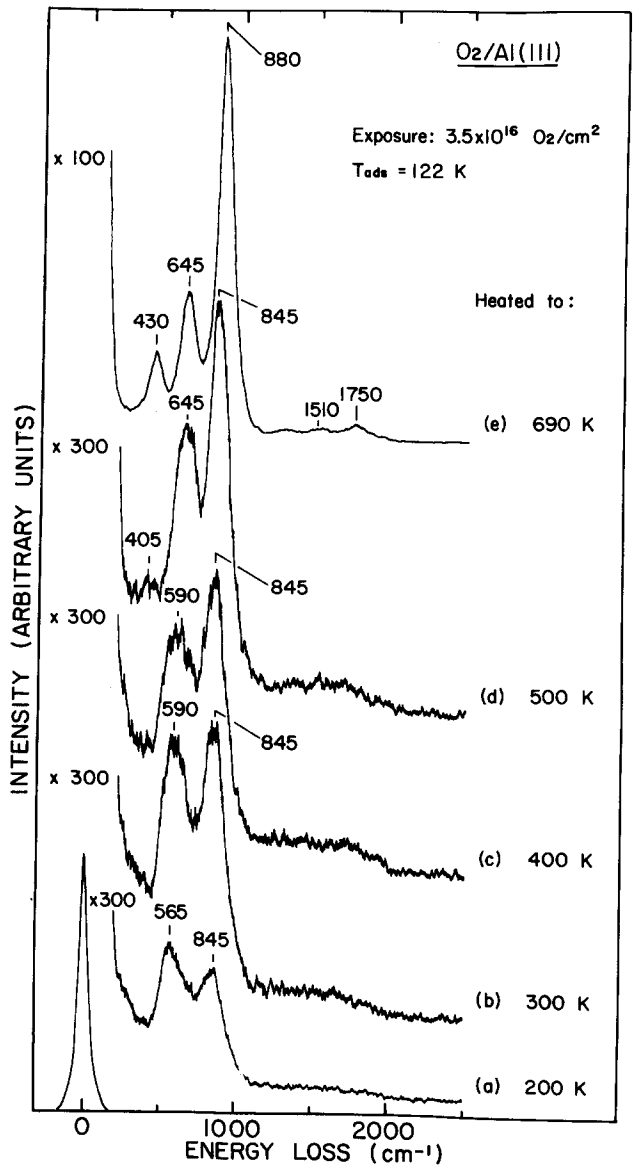

Fig. 6. Vibrational spectra of oxygen adsorption on Al(111) followed by heating to the indicated temperature. All spectra were measured between 122 and 140 K.

O–Al(111) system (fig. 6). Another change observed in fig. 7 (with increasing temperature) is that as the 1470 cm^{-1} mode decreases, it becomes broader and its peak frequency shifts to 1500 cm^{-1}. The width (FWHM) of this peak is 81

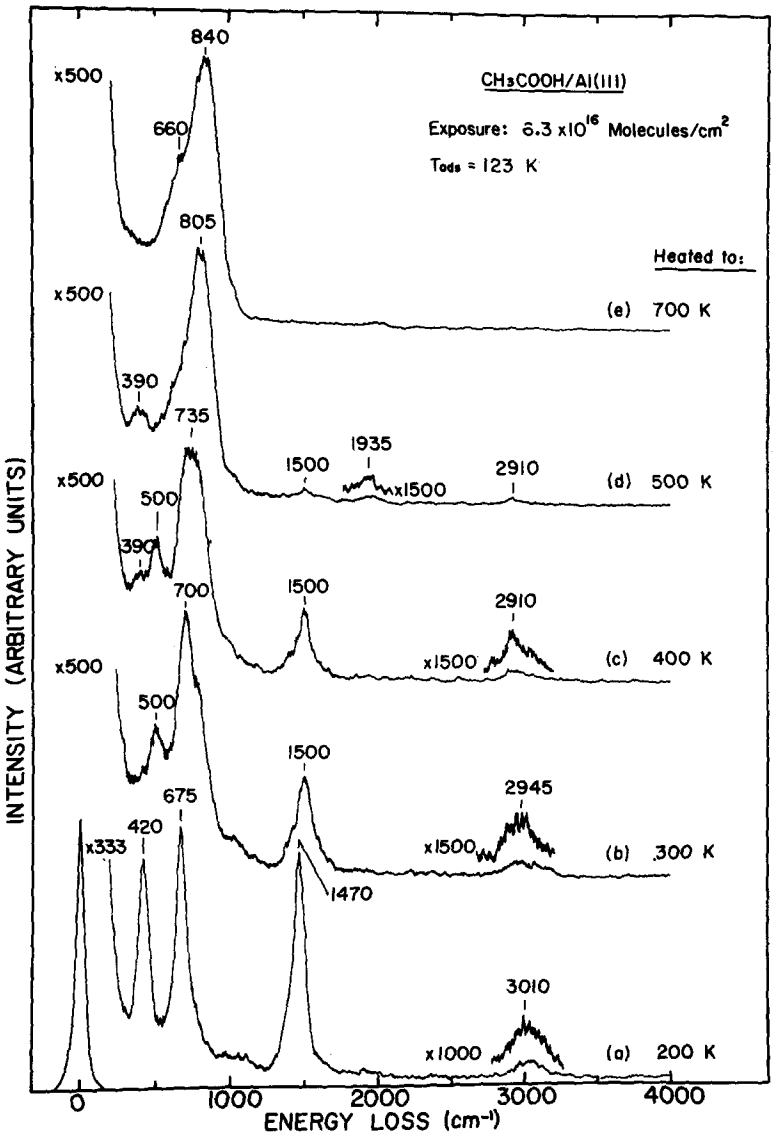

Fig. 7. Vibrational spectra of an adsorbed acetate layer on Al(111) recorded as a function of temperature.

cm^{-1} at 200 K (spectrum a), but increases to 160 cm^{-1} following heating to 300 K (spectrum b), while the widths of the elastic peaks for those two spectra remain constant at 61 cm^{-1}.

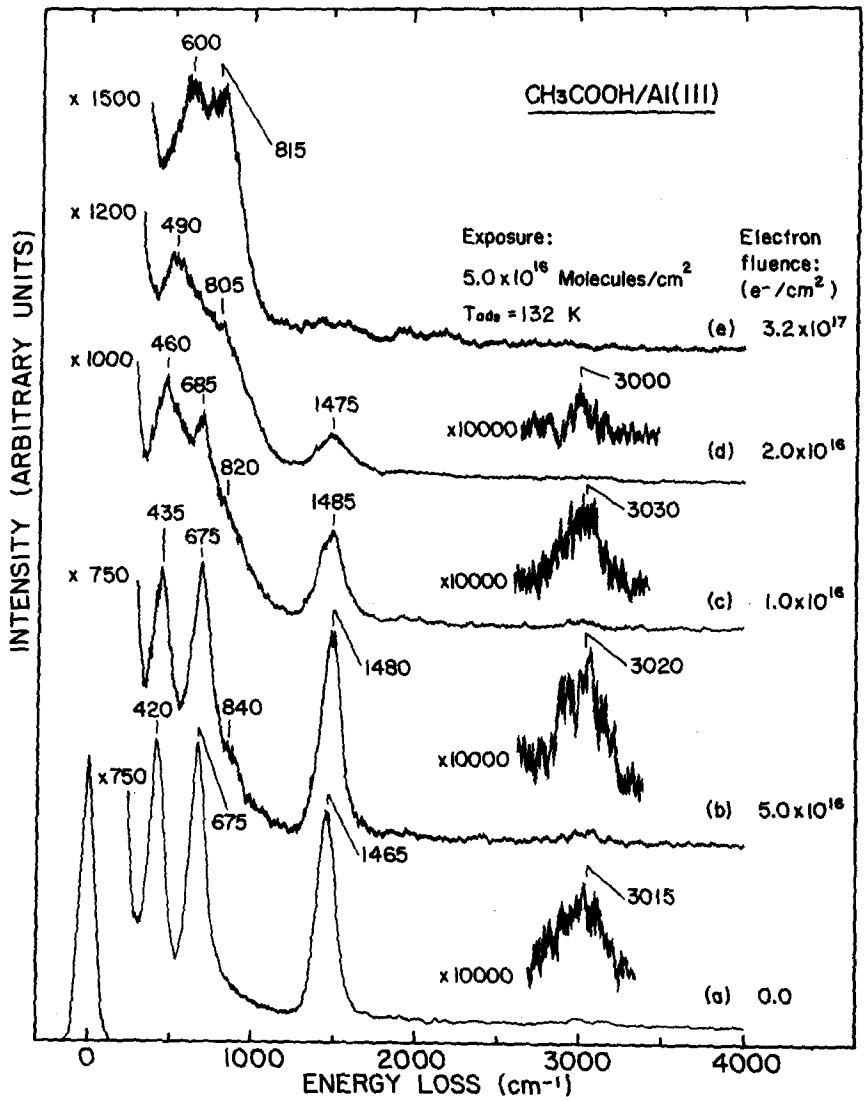

Fig. 8. Electron stimulated decomposition of an adsorbed acetate layer on Al(111).

3.3. The effect of electron irradiation

A series of EEL spectra recorded as a function of electron fluence upon an adsorbed layer produced from acetic acid on the Al(111) surface are shown in fig. 8. The layer was prepared at a CH_3COOH exposure of 5.0×10^{16} molecules/cm^2 at 132 K. Spectrum 8a was collected before any electron irradiation,

while the subsequent spectra were measured after the adsorbed layer was electron bombarded to the indicated value. A broad uniform 300 eV electron distribution was emitted from a 1.8 cm diameter W spiral made of 0.025 cm diameter wire. All EELS measurements and electron bombardment were performed at a measured crystal temperature below 200 K. As seen in fig. 8, one observes a gradual decrease of the loss features related to the adsorption of acetic acid, and the simultaneous development of new vibrational modes in the energy region below 1000 cm^{-1} with increasing electron irradiation. At an electron fluence of 3.2×10^{17} e^-/cm^2 (fig. 8e), a spectrum with only loss features at 600 and 815 cm^{-1} is obtained. This spectrum is similar to that obtained from the adsorption of O_2 on Al(111) at 200 K (fig. 6a), and differs significantly from the vibrational spectrum for Al_2O_3 (fig. 6e).

4. Discussion

4.1. Formation of acetate on Al(111) at 120 K

As shown in figs. 1 and 2, at low acetic acid exposures ($\leqslant 6.3 \times 10^{16}$ molecules/cm^2), the adsorption of either CH_3COOH (figs. 1a and 1b) or CD_3COOH (figs. 2a and 2b) on a clean Al(111) surface at 120 K produces similar EEL spectra except for the frequency shift of ν(CH) at 3010 cm^{-1} to ν(CD) at 2285 cm^{-1}. The absence of any O–H stretching vibration in the spectra suggests that the acetic acid undergoes O–H bond scission upon adsorption on Al(111) at 120 K, resulting in the formation of an adsorbed acetate species. The comparison given in table 1 of the vibrational frequencies observed for the surface species on Al(111) with those of acetate ion in aqueous solution [11] and adsorbed acetate on Cu(100) [3] confirms that the acetate species does form on Al(111) even at this low temperature. By

Table 1
Comparison of vibrational frequencies (in cm^{-1}) of aqueous acetate ion [11] and acetate on Cu(100) [3] with those observed for surface species on Al(111)

Mode	CH_3COO^- (CD_3COO^-) [a]	Cu(100) [b]	Al(111) [c]
ν(M–O)	– –	339 (308)	425 (410)
δ(OCO)	650 (619)	677 (648)	675 (655)
ν(C–C)	926 (883)	1041 (1061)	1055 (1070)
$\delta(CH_3)$	1344 (1085)	– –	– –
ν_s(COO)	1413 (1406)	1434 (1413)	1470 (1470)
ν_a(COO)	1556 (1545)	– –	– –
ν(CH)	2935 (2111)	3000 (2218)	3025 (2260)

[a] Ref. [11].
[b] Ref. [3].
[c] This work.

comparing the frequencies shown in table 1, the assignment of the vibrational transitions observed for surface acetate on Al(111) is readily given as, ν(Al–O) at 425 cm^{-1}, δ(OCO) at 675 cm^{-1}, ν(C–C) at 1055 cm^{-1}, ν_s(COO) at 1465 cm^{-1}, and ν(CH) at 3010 cm^{-1}.

The observation of an intense ν(Al–O) bond indicates that the acetate species is bonded to the Al(111) surface *via the oxygen end of the molecule*. Important information is readily ascertained from the absence of the ν_a(COO) mode in the EEL spectra representative of the adsorbed acetate, considering that this mode has an intensity comparable to that of the ν_s(COO) band for the free acetate ion. This information is derived from the surface dipole selection rule: namely, only those vibrations which belong to the totally symmetric representations, A, A_1, and A′ of the point group describing the symmetry of the surface complex, are observable as fundamentals in dipole scattering [12]. The ν_a(COO) mode will not be observed on-specular if the acetate species has a C_s symmetry, since in this symmetry it belongs to an irreducible representation of A″. The absence of the ν_a(COO) band in figs. 1b and 2b thus suggests that the acetate, produced from acetic acid exposure at 120 K, chemisorbs with C_s symmetry with symmetric bonding of the oxygen atoms to the surface and identical Al–O bonds. The local symmetry of the OCO moiety is C_{2v}, with the methyl group symmetrically attached to the carbon atom, resulting in an overall acetate symmetry of C_s.

The formation of surface acetate species on the clean Al(111) crystal directly upon exposure to acetic acid at 120 K is quite unique compared to that observed on transition metal surfaces [1–3]. At low temperatures (< 225 K), acetic acid adsorbs strictly in a molecular form on these metal surfaces. Only on oxygen pre-dosed transition metal surfaces is the formation of an acetate species observed at these low temperatures. It is believed that the pre-adsorption of oxygen enhances the Bronsted basicity of the metal surface [1]. The observation of acetate formation on Al(111) at 120 K thus indicates the relatively strong basicity and reactivity of aluminum surfaces toward this class of organic molecules, with the molecular site for reactivity being the oxygen and the hydroxyl moiety in CH_3COOH.

4.2. Molecular adsorption of acetic acid at 120 K

Molecular adsorption of the acetic acid occurs only after the acetate layer has been saturated as indicated in figs. 1 and 2. Initially, only the intensity of the acetate vibrational features change with increasing exposure, as more acetic acid molecules react with Al(111) to produce adsorbed acetate. When the CH_3COOH exposure exceeds 9.5×10^{16} molecules/cm^2 (figs. 1c and 1d), new features in addition to those of acetate emerge. The development of vibrational transitions at similar energies are also observed at higher CD_3COOH exposures (figs. 2c and 2d), with the appearance of an additional

feature at 1050 cm^{-1}. The presence of a mode at 3010 cm^{-1}, namely ν(C–H), for high exposures to CD_3COOH in fig. 2d is likely due to facile hydrogen isotope exchange on the surface and in the metal dosing system. The involvement of residual gas phase H_2 cannot be excluded, and slight hydrogen impurity in the labeled CD_3 groups may also be involved. The new frequencies observed in figs. 1 and 2 for acetic acid layers on top of chemisorbed acetate are compared with those of gas phase acetic acid [13] as given in table 2. The assignment of these features to molecular acetic acid is unequivocal based on the frequency shift for specific modes upon partial deuteration. The very intense loss feature at 1450 cm^{-1} in fig. 1d is attributed to the overlap of ν_s(COO) mode of the underneath acetate (1465 cm^{-1}) with $\delta(CH_3)$ of the molecular acetic acid, based on the observation of a strong $\delta(CD_3)$ band at 1050 cm^{-1} at higher CD_3COOH exposures (fig. 2d).

The vibrational energy of the ν(OH) mode, 2740 cm^{-1}, is unusually low. This is due to dimer formation and OH $\cdots$ O bonding of the physisorbed acetic acid multilayer. According to the results presented by Schoofs et al. [4], the acetic acid vapor is in the dimeric form under the dosing conditions we have used (i.e. an acetic acid pressure of 10 Torr behind the pinhole orifice at a gas temperature of ca. 300 K). The adsorption of acetic acid dimers on the acetate-covered Al(111) surface is supported by the frequency given by Bellamy [14], who indicates that the ν(OH) mode should appear in the energy range of 2700–2500 cm^{-1} for carboxylic acid dimers. In addition, the broad feature at $\approx$ 950 cm^{-1}, which is observed for the adsorption of CH_3COOH and CD_3COOH on Al(111) at high exposures (figs. 1d and 2d), is a perturbed δ(OH) mode characteristic of the dimeric form and is not found at this low an energy for the monomeric acid [10], as shown in table 2. Hence, dimer formation is observed upon condensation of the molecular acid because, under the conditions used here, we are dosing essentially acetic acid dimers. However, we do not expect to see a substantial difference in the chemical behavior of the Al(111) surface toward the monomeric acetic acid form. The reactivity

Table 2
Comparison of acetic acid vapor vibrational frequencies (in cm^{-1}) [13] with surface species on Al(111)

Mode	CH_3COOH (g) (CD_3COOH)(g) [a]	Al(111) [b]
δ(OH)	1186 (1156)	990 (945)
ν(C–O)	1282 (1220)	1350 (1310)
$\delta(CH_3)$	1387 (1075)	1400 (1050)
ν(C=O)	1739 (1730)	1730 (1730)
ν(O–H)	3125 (3106)	2740 (2740)
ν(C–H)	3030 (2128)	3030 (2275, 2155)

[a] Ref. [13].
[b] This work.

of the aluminum surface toward acetic acid is very strong, as indicated by the formation of acetate at 120 K upon initial exposure of the dimer. We would expect to observe the same OH scission process for the dimeric and monomeric acetic acid species.

4.3. Thermally induced decomposition

As discussed above, at higher acetic acid exposures, the molecular acid condenses on top of the adsorbed acetate layer. The TPD results for such an adsorption system (fig. 3) show a number of masses (m/e ratios) with desorption peaked at 167 K. The fact that they all occur simultaneously indicates that they result from the desorption of a single adsorbed species. Line of sight analysis of the dosed CH_3COOH vapor reveals that all of the masses shown in this figure, 60, 45, 43, 16, 15 and 2 amu are either the parent feature or major spectrometric cracking fragments of gaseous acetic acid. In addition, the relative *intensity ratios* observed in fig. 3 are in good agreement with those found for CH_3COOH vapor. The TPD results shown in fig. 3 thus indicate that the physisorbed acetic acid desorbs molecularly with a desorption rate maximum at 167 K.

Molecular desorption also occurs at lower acid exposures as evident from the 43 amu fragment observed in fig. 4A. However, the peak intensity ratios observed from this overlayer are different than the cracking pattern observed for the vapor. In addition, the shapes of the 15 and 16 amu thermal desorption states are similar, yet both obviously different from the shape of the 43 amu feature, as shown in the inset in fig. 4A. Hence, the relatively strong peak intensities of the masses at 16, 15 and 2 amu, combined with the obvious difference in their peak shapes to that of the 43 amu desorption state suggest that, in addition to desorption of the physisorbed acetic acid, partial decomposition of either the adsorbed acetate or adsorbed acetic acid also occurs in this temperature range. The desorption/decomposition of the multilayer acetic acid at ≈ 167 K is also confirmed by the corresponding EELS results as shown in fig. 5. After the surface was heated to 200 K (fig. 5b), the vibrational modes related to the molecular acetic acid [i.e. ν(OH), ν(C=O) and δ(OH)] disappear compared to the spectrum collected after adsorption of acetic acid at 120 K (fig. 5a).

Fig. 5b is a representative spectrum of the adsorbed species present on the Al(111) surface after the desorption/decomposition of the molecular acid. Comparing the vibrational frequencies observed in this spectrum with those of the free acetate ion as given in table 1, one can readily assign this adsorbed species to the surface acetate. The difference between the acetate species produced by heating a condensed layer (fig. 5b) and by initial CH_3COOH exposure at 120 K (fig. 1b) is the appearance of two new features, a mode due to overlapping of the C–C stretching and CH_3 rocking modes at about 1050

cm^{-1}, and ν_a(COO) at 1615 cm^{-1}, respectively, as well as a greatly enhanced relative intensity of the ν(CH) mode at 3025 cm^{-1}. Since the ν_a(COO) mode is dipole forbidden if the adsorbed acetate is in C_s symmetry, the observation of this mode indicates that the surface complex now has a C_1 symmetry. In addition, the acetate layer produced upon heating a condensed layer to 200 K (fig. 5b) has new features between 350 and 750 cm^{-1} which partially obscure the sharp ν(Al–O) and δ(OCO) features of the adsorbed acetate (cf. figs. 5b and 1b). Our previous study of the interaction of O_2 with Al(111) [8,15] has shown that atomic O–Al vibrational motions also appear in the 500–1000 cm^{-1} region as evident in fig. 6a. The substantial changes of the peak shapes in the energy region below 1000 cm^{-1} in fig. 5b indicate the presence of adsorbed oxygen atoms after the desorption/decomposition of the condensed acetic acid. The lowering in symmetry of the adsorbed acetate from C_s to C_1, as well as the presence of coadsorbed oxygen atoms on the acetate-covered Al(111) surface were also observed at appropriately shifted frequencies upon heating a condensed CD_3COOH layer to 200 K. This lowering in symmetry of the surface acetate species can be attributed to one of two possible factors: (1) the presence of coadsorbed oxygen incorporated into the Al lattice (see below) lowers the symmetry of the acetate–surface complex, or (2) partial decomposition of the adsorbed layer leads to distortion of a significant fraction of the undecomposed acetate to C_1 symmetry.

In a previous study we have thoroughly investigated the adsorption of oxygen on an Al(111) surface [8]. From this study we concluded that the two vibrational transitions observed at 200 K in fig. 6a are due to a surface O–Al stretching motion (565 cm^{-1}) and a subsurface O–Al vibrational motion (845 cm^{-1}), respectively. Heating this layer increases the degree of incorporation of the oxygen atoms from the surface to subsurface binding sites and eventually leads to the formation of aluminum oxide at higher temperatures [8]. The corresponding spectral changes for the oxygen–aluminum system include a progressive increase in the relative intensity of the subsurface O–Al (845 cm^{-1}) stretching mode, combined with a gradual frequency shift to higher energy of both vibrational transitions.

Heating the adsorbed layer present after the desorption/decomposition of the condensed acetic acid (fig. 5) shows spectral changes at energies below 1000 cm^{-1} similar to those observed for heating an oxygen-dosed Al(111) surface. The growth in loss intensity and the shift in peak frequency observed between 200 and 500 K clearly arise from incorporation of oxygen into the Al lattice caused by dissociation of adsorbed acetate. Some decomposition has already occurred by 200 K, as indicated above, but continues with further heating. The majority of the acetate decomposition for this saturated layer does not occur, however, until temperatures exceed 500 K. The resulting surface layer produced upon heating to 700 K shows no loss features characteristic of adsorbed acetate and displays Auger transitions characteristic of

carbon, oxygen and aluminum oxide (54 eV). The loss features in fig. 5e are much broader than the sharp oxide spectrum shown in fig. 6e; this difference is likely due to the overlap of the O–Al stretching modes with Al–C vibrational modes, which also have vibrational transitions in the 400–700 cm^{-1} energy region [16].

A similar thermal decomposition sequence was observed for a pure acetate layer prepared by a relatively low CH_3COOH exposure at 123 K, as shown in fig. 7. The decomposition of adsorbed acetate is similarly accompanied by the simultaneous formation of surface and subsurface Al–O species. A closer inspection of fig. 7 reveals that, in addition to a decrease of acetate loss features with heating, the ν_s(COO) mode at 1470 cm^{-1} significantly broadens and shifts in frequency to 1500 cm^{-1}. This fact is likely due to the overlap of the ν_s(COO) mode at 1470 cm^{-1} with $\delta(CH_3)$ and ν_a(COO) acetate modes at 1345 and 1615 cm^{-1}, respectively. The observation of a ν_a(COO) mode is expected if heating causes a reduction in symmetry of a portion of the undecomposed acetate species. As discussed above, a reduction to C_1 symmetry of the acetate–surface complex can occur upon oxygen incorporation into the Al lattice or simply from distortion of the acetate species resulting in loss of the mirror plane symmetry.

The broadening of this ν_s(COO) mode in fig. 7, combined with the relatively strong ν(CH) mode at $\approx$ 3010 cm^{-1} observed in fig. 5 might also be caused by production of a CH_3(a) species upon the decomposition of adsorbed acetate. However, such a species is expected to have strong vibrational transitions at 1208 and 1437 cm^{-1} (symmetric and asymmetric methyl deformation modes) as observed for $(CH_3)_6Al_2$ [17]. Based on the absence of the 1208 cm^{-1} mode in figs. 5 and 7, as well as the lack of loss features at 955 and 1140 cm^{-1} in the CD_3COOH EEL spectra for the same heating sequence (not shown), we do not believe this species exists during the decomposition of adsorbed acetate on the Al(111) surface. However, we cannot rule out the formation of CH or CH_2 species (viz. CH, CCH, CH_2 or CCH_2), as these species would have strong transitions at ca. 800 cm^{-1} (CH bonding mode) or ca. 1400 cm^{-1} (CH_2 scissor mode), respectively [18]. The presence of these modes would also be obscured by the oxide and acetate features upon deuteration.

A noticeable difference between the thermal decomposition of the acetate species produced upon heating a condensed acetic acid layer to 200 K (fig. 5) and upon low exposure to acetic acid at 123 K (fig. 7) is the retardation of surface decomposition on surfaces derived from multilayer coverages. In fig. 5 (from multilayer acetic acid), a significant amount of acetate still exists on the surface even after the crystal is heated to 500 K, while the decomposition process is almost complete at the same temperature for an adsorbed layer with a lower acetate coverage (fig. 7). Such a coverage-dependent decomposition behavior of surface acetate, (i.e., increasing the initial acetate coverage de-

creases the decomposition rate) has been observed on Pt and Ni transition metal surfaces [1,4]. This is attributed to the attractive interactions between the adsorbed acetate species, enhancing their stability and raising the activation energy for thermal decomposition of the surface acetate [4]. It may also be due to diminished availability of unfilled Al sites needed for decomposition in the multilayer-generated surface layer.

This observation may also be attributed to the formation of oxide on Al(111), since generally the reaction intermediates are more stable on oxygen-modified metal surfaces than on clean metal surfaces. The higher stability of the multilayer-derived acetate may be due to the formation of a sufficient amount of oxide upon the desorption/decomposition of the physisorbed acetic acid at 167 K (see fig. 5b), while the lower stability of the submonolayer-derived acetate may be the result of incomplete or insufficient oxide formation.

The different decomposition rate for these two layers, as indicated by the EEL spectra, is curiously not reflected in the TPD results (fig. 4). The evolution of H_2, the only detectable thermal decomposition product of acetate, occurs at the same temperature as shown in figs. 4A and 4B, respectively. This suggests that the desorption of H_2 from the Al(111) surface is a desorption-limited process. The H atoms on and/or near the surface, produced by the decomposition of the acetate, do not evolve as H_2(g) until the crystal temperature reaches 540 K. The weak feature at 1935 cm^{-1} in fig. 7d is characteristic of an Al–H stretching vibration [19], which confirms the presence of adsorbed H atoms on the Al(111) surface at 500 K. The absence of this ν(Al–H) mode in the other EEL spectra in fig. 7 may be due to the fact that this ν(Al–H) mode is only visible when the surface hydrogen concentration reaches a significant level.

The TPD, EELS and AES results of the effect of temperature on acetate adsorbed on Al(111) suggest that the decomposition pathway is controlled by the scission of C–O and C–C bonds, accompanied by the formation of Al–O and Al–C surface species. The lack of CO and CO_2 as thermal decomposition products, combined with the absence of any stable decomposition intermediates in the EEL spectra other than acetate, indicates the strong reactivity and affinity of aluminum surfaces toward oxygen and carbon incorporation.

4.4. Electron stimulated decomposition

Electron irradiation results in the decomposition of adsorbed acetate on Al(111), as evident in fig. 8. Upon electron bombardment, one observes a progressive decrease of the acetate features and a gradual development of the surface and subsurface O–Al loss features. After an electron fluence of 3.2×10^{17} e^-/cm^2 (fig. 8e) the decomposition of the acetate is complete, resulting in a vibrational spectrum similar to that obtained for the O–Al(111)

system at 200 K (fig. 6a). AES analysis reveals that this layer contains both carbon and oxygen adsorbed on the Al(111) surface.

The decomposition of the adsorbed acetate induced either by heating (fig. 7) or by electron irradiation (fig. 8) occurs in a similar manner. The only discernable difference between thermal and electron induced decomposition is the nature of the resulting O–Al(111) layers (cf. figs. 7e and 8e). We have shown in fig. 6 that, for an O–Al(111) system, heating increases the incorporation rate of oxygen atoms and thus enhances the intensity of the higher frequency mode (i.e., the subsurface O–Al vibrational motion at ca. 840 cm^{-1}). Since the ESD experiments were performed at temperatures below 200 K, the EEL spectrum of the resulting O, C–Al(111) surface is more like that of an O–Al(111) layer produced at low temperatures (fig. 6a), where extensive O-penetration has not occurred. On the other hand, heating the acetate layer always produces a vibrational spectrum with oxygen features similar to that obtained for the O–Al(111) system heated to a similar temperature (fig. 6e). The ESD results thus confirm that the decomposition pathway of the adsorbed acetate is controlled by scission of C–O and C–C bonds and the simultaneous formation of Al–O and Al–C bonds on the Al(111) surface.

5. Conclusions

From the above results and discussion of the interaction of acetic acid with Al(111), one can conclude that aluminum has a unique surface chemistry toward carboxylic acids compared to transition metal surfaces:

(1) Acetic acid reacts with an Al(111) surface at 120 K to form surface acetate species. Aluminum surfaces have relatively strong reactivity and affinity toward oxygen and therefore break the O–H bond of the acid even at this low temperature.

(2) The adsorbed acetate at 120 K is symmetrically bonded to Al(111) with a C_s surface point group symmetry.

(3) Molecular acetic acid condenses at 120 K only after saturation of the surface acetate layer. The condensed multilayer is in a molecular dimer form.

(4) The condensed layer desorbs from the surface at about 167 K, leading to reduction in symmetry of the adsorbed acetate (C_1 symmetry) and production of adsorbed oxygen on the Al(111) surface.

(5) The thermal decomposition of the adsorbed acetate is coverage dependent. The decomposition evolves H_2 and produces a surface covered with both oxygen and carbon. The decomposition pathway is controlled by the scission of C–O and C–C bonds, with the simultaneous formation of Al–O and Al–C bonds.

(6) Electron irradiation induces complete decomposition of the adsorbed acetate on an Al(111) surface, eventually producing adsorbed oxygen and carbon.

Acknowledgements

We acknowledge with thanks the support of this work by the Aluminum Corporation of America (ALCOA). We also thank Dr. Karl Wefers of ALCOA for helpful discussions and for suggesting this problem. J.G. Chen acknowledges the support of the A.W. Mellon Educational and Charitable Trust in the form of an Andrew Mellon Predoctoral Fellowship.

References

[1] N.R. Avery, J. Vacuum Sci. Technol. 20 (1982) 592.
[2] B.A. Sexton, J. Vacuum Sci. Technol. 17 (1980) 141.
[3] B.A. Sexton, Chem. Phys. Letters 65 (1979) 469.
[4] G.R. Schoofs and J.B. Benziger, Surface Sci. 143 (1984) 359.
[5] M. Bowker and R.J. Madix, Appl. Surface Sci. 8 (1981) 299.
[6] J.P. Batra and L. Kleinman, J. Electron Spectrosc. Related Phenomena 33 (1984) 175.
[7] J.W. Rogers, Jr., R.L. Hance and J.M. White, Surface Sci. 100 (1980) 388.
[8] J.E. Crowell, J.G. Chen and J.T. Yates, Jr., Surface Sci. 165 (1986) 37.
[9] R.J. Muha, S.M. Gates, J.T. Yates, Jr. and P. Basu, Rev. Sci. Instr. 56 (1985) 613.
[10] S.M. Gates, J.N. Russell, Jr. and J.T. Yates, Jr., Surface Sci. 146 (1984) 199.
[11] K. Ito and H.J. Bernstein, Can. J. Chem. 34 (1956) 170.
[12] H. Ibach and D.L. Mills, Electron Energy Loss Spectroscopy and Surface Analysis (Academic Press, London, 1982).
[13] R.C. Herman and R. Hofstadter, J. Chem. Phys. 6 (1938) 534; 7 (1939) 460.
[14] L.J. Bellamy, The Infrared Spectra of Complex Molecules (Chapman and Hall, London, 1975).
[15] J.G. Chen, J.E. Crowell and J.T. Yates, Jr., Phys. Rev. B. 33 (1986) 1436.
[16] J. Yamamoto and C.A. Wilkie, Inorg. Chem. 10 (1971) 1129.
[17] A.P. Gray, Can. J. Chem. 41 (1963) 1511;
T. Ogawa, Spectrochim. Acta 24A (1968) 15.
[18] B.E. Koel, J.E. Crowell, B.E. Bent, C.M. Mate and G.A. Somorjai, J. Phys. Chem., in press.
[19] P.A. Thiry, J.J. Pireaux, M. Liehr and R. Caudano, J. Vacuum Sci. Technol. A3 (1985) 1439.